A tapered parallel-plate-waveguide probe for THz near-field reflection imaging

Jingbo Liu,[1] Rajind Mendis,[1,a)] Daniel M. Mittleman,[1] and Naokazu Sakoda[2]
[1]*Department of Electrical and Computer Engineering, MS-378, Rice University, Houston, Texas 77005, USA*
[2]*Kobe Steel, Ltd., Kobe, Hyogo, Japan*

(Received 17 November 2011; accepted 23 December 2011; published online 17 January 2012)

We demonstrate a broad-band low-loss THz near-field imaging technique based on a tapered parallel-plate waveguide. This technique works in a reflection geometry, which avoids the problem of low energy throughput due to the impedance mismatch and consequently limited spatial resolution, in the transmission geometry. Images reconstructed by the filtered-back-projection algorithm are able to resolve features of size $\sim$100 μm using radiation with an average wavelength of 1.5 mm. © *2012 American Institute of Physics*. [doi:10.1063/1.3677678]

Over the last few years, there has been continuous interest in broadband THz near-field imaging. In order to overcome the diffraction-based resolution limit, a variety of aperture-based and apertureless raster-scanned near-field imaging techniques have been explored.[1–3] For broadband sub-wavelength imaging, the propagation loss and dispersion continue to pose significant challenges and limit the applicability of THz near-field techniques.[4] One possible candidate for a near-field probe which addresses these concerns is the tapered parallel-plate waveguide (PPWG). The PPWG has proven to be an excellent platform for many THz applications in the last decade.[5] Recently, a PPWG with a small plate spacing was used as a line-illumination probe for broad-band THz near-field imaging.[6] In this work, the signals transmitted through the waveguide and sample were used to reconstruct sub-wavelength images using a filtered-back-projection algorithm. However, according to transmission line theory, the impedance mismatch between the waves inside the waveguide and the waves in free space increases as the plate spacing decreases. In fact, for parallel plates, the amplitude of the transmitted radiation decreases approximately as the ratio b/λ, where b is the plate spacing.[7] This limits the resolution and throughput for this transmission-mode imaging technique.

Within the last 3 years, sub-wavelength confinement of broadband THz pulses has been studied both theoretically[8] and experimentally.[9,10] This spacing-tapered technique starts from a relatively large input plate spacing and gradually compresses the propagating THz waves into smaller scales. This spacing-tapered PPWG has the advantage of eliminating input energy coupling limitations, for example, for spectroscopic measurements.[11,12] In this report, we use a tapered PPWG as a probe in *reflection* mode, for near-field imaging. Using the reflected wave, rather than relying on the transmitted wave, permits us to avoid the concerns associated with the large wave impedance mismatch, and therefore achieve better spatial resolution and an improved signal-to-noise (S/N) ratio. Similar techniques have been demonstrated at millimeter wave frequencies.[13,14]

The experimental set-up consists of a THz-TDS system, with the fiber-coupled transmitter and receiver positioned as shown in Fig. 1. The transmitter and receiver are situated close to the focal plane of a teflon lens that has a focal length of 6 cm. The tilt angle between the transmitter and receiver is 10°. An aluminum-foil shield is located between the transmitter and receiver to block any interference between them. In order to excite the TEM mode in the PPWG, the input THz waves are polarized perpendicular to the waveguide plates. A plano-cylindrical teflon lens of 1.2 cm radius and 4 cm length is used to couple the incident THz waves into the waveguide and also couple the reflected waves out of the waveguide. The PPWG has a width of 5 cm and a spacing tapered from a large size ($\sim$1.5–2 mm) at the input facet to a much smaller size ($\sim$20–100 μm) at the output facet, within a propagation length of 2.5 cm. This tapered PPWG transfers the broad-band waves into the sub-wavelength output facet, so that it can serve as a near-field probe with the resolution determined by the output spacing size.[6,9,10] The imaging sample mounted on a rotation stage coupled to a translation stage is placed in close proximity (down to $\sim$20 μm) to the output facet of the waveguide. The two motion-control stages are used to scan the sample position relative to the waveguide. The measured data are then used to reconstruct the images by the filtered-back-projection algorithm.[6,15]

First, we characterize the reflected signal in various situations. The sub-wavelength aperture at the output facet of the PPWG results in a wave impedance mismatch between the propagating waves inside the waveguide and that of the near field outside the waveguide. This leads to a reflection of the propagated signal back into the waveguide.[7,16,17] We measure the reflected signal from the output face for three cases: an untapered PPWG with a spacing of 2 mm, the same untapered PPWG with a mirror closely attached to the output face, and a PPWG with the spacing tapered from 2 mm to 200 μm. For the untapered PPWG without the mirror, the reflection is nearly zero as expected. We note that the broad-band reflection from the tapered PPWG [solid line in Fig. 2(a)] is comparable in amplitude to the reflection from the mirror at the end of the untapered PPWG [dashed line in Fig. 2(a)]. Thus, this tapered PPWG probe reflects most of the input signal, making it feasible to work in reflection

a)Author to whom correspondence should be addressed. Electronic mail: rajind@rice.edu.

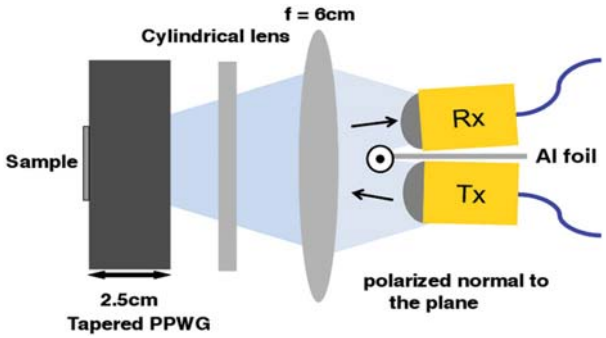

FIG. 1. (Color online) Schematic of the experimental setup.

mode. We also note that there is some low-pass filtering in the reflected signal caused by the impedance mismatch, which can be readily understood by the b/λ throughput that we mentioned earlier. Furthermore, the fact that these two signals are comparable is a good indication of the higher S/N ratio that is achievable in the reflection geometry compared to a transmission one, at these small output plate separations.

Next, we consider the effect of a flat object (made of glass, silicon, or aluminum) situated at the waveguide output. We taper the PPWG spacing from 1.5 mm to 20 μm and consider the change in the reflection coefficient induced by an object placed in close proximity ($\sim$20 μm) to the output facet. Due to the higher refractive index compared to air, this object modifies the impedance mismatch and leads to a change in the reflection. This change in the reflection depends on the distance from the object to the output facet, as shown in Fig. 2(b). We note that in our experiment, it is not possible to have the object exactly in contact with the very edge of the probe due to practical considerations. The closest possible distance between the object (substrate) and the output facet of the tapered PPWG is $\sim$20 μm. Counter intuitively, at this distance, we do not observe a perfect mirror-reflection from the aluminum object. This is better understood via numerical simulations of the physical problem using the finite-element method. These results, shown in Fig. 2(c), reproduce our measurements qualitatively, indicating a turning point in the curve as the object is brought closer. To understand this further, we could imagine that when the object is 20 μm away from the output facet, it forms a waveguide T-junction with the 20 μm plate spacing at the output facet. This could help to guide energy out of the waveguide along the output facet, leading to the observed drop in the amplitude of the reflected signal. We note that in our simulation, when the aluminum object is in perfect contact with the output facet, there is an almost 100% reflection, as expected.

When the object is moved further away from the output facet, there is less disturbance to the near field, and a much stronger reflection results. The reflection keeps increasing until the distance is about 0.1 mm and results in a relatively stable reflection beyond this point. Based on this result, a topographic feature on a sample of height 0.1 mm or less could be identified by the change in the reflection. This change is due to the disturbance to the waves in the near field, which extends from the end of the waveguide to a distance roughly equal to the waveguide gap[15,16] We also note

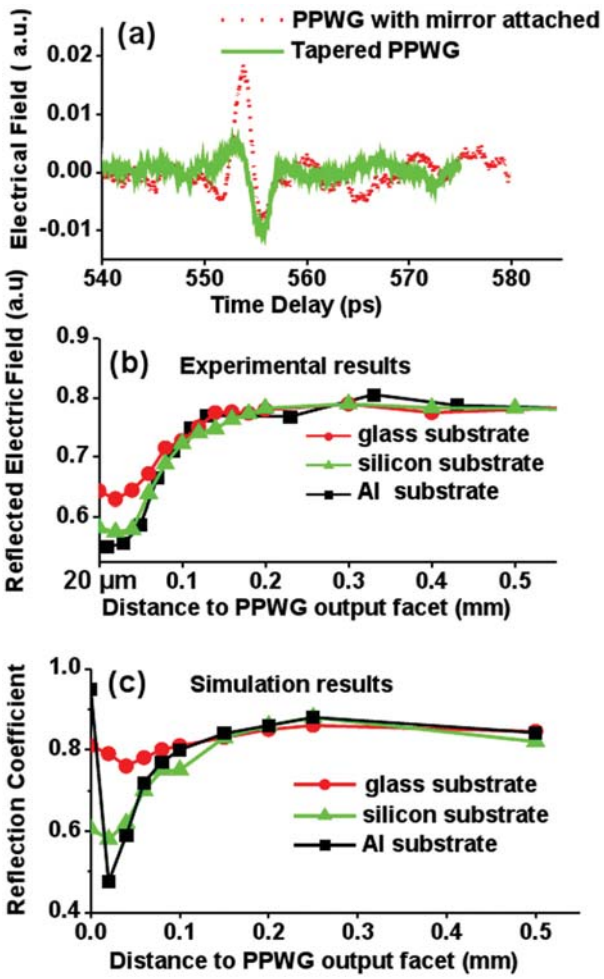

FIG. 2. (Color online) (a) Time-domain reflections from an untapered PPWG of plate spacing 2 mm with attached mirror and from a PPWG with tapered plate spacing, from 2 mm to 200 μm. (b) Measured reflected electric field as a function of sample distance to the waveguide output facet, for glass, silicon, and aluminum (flat) samples. (c) Simulated reflection coefficients corresponding to the configurations in (b).

that in both Figs. 2(b) and 2(c), at any particular distance within the transient regime, the reflected signal differs for different substrate materials. Therefore, the tapered-PPWG probe in reflection mode is able to differentiate both topographic features and dielectric properties of the sample.

To investigate the imaging capabilities, we used a sample consisting of a gold pattern on a GaAs substrate, as shown in Fig. 3(a). This sample is essentially flat (within $\sim$100 nm), so, no topographic information is retrieved. However, we show that it is possible to obtain information based on the dielectric contrast. We scan the sample across the tapered PPWG output facet in a direction normal to the plates (x direction). The spacing at the output facet of the tapered-PPWG probe and its proximity to the sample determine the best resolution this imaging technique can achieve.[4] This tapered PPWG gives high resolution only in one direction: the direction normal to the plates. To obtain a two-dimensionally resolved image, a linear scan (x-scan) alternating with a rotational scan of the sample was carried out based on the filtered-back-projection (FBP) approach. The maximum length on the sample is $\sim$4.5 mm, so, the linear scan range is 0–9 mm with a step size of 20 μm, to make

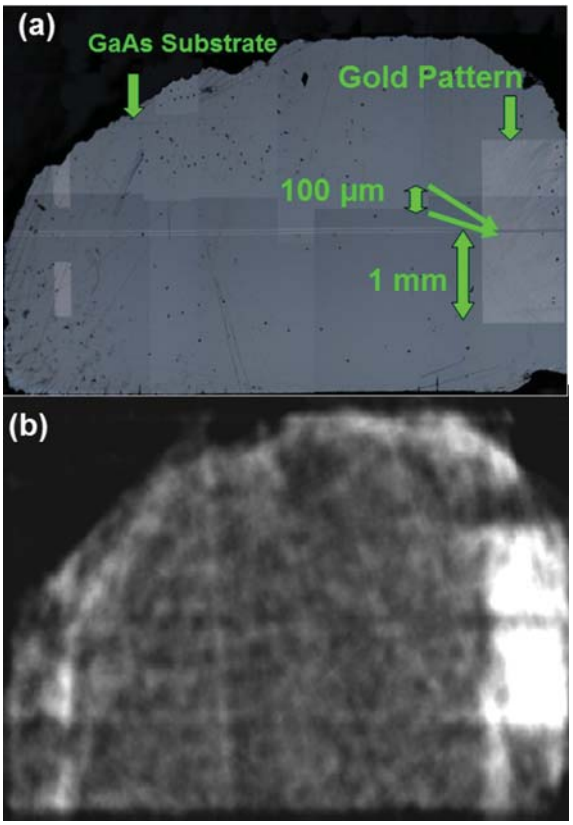

FIG. 3. (Color online) (a) Sample image under optical microscope. (b) Reconstructed sample image by the filtered back projection algorithm.

sure the complete sample area is covered. The rotational scan is around the optical axis from 0° to 175° with a step angle of 5°. In total, 16 236 projection time-domain signals were recorded, and each signal has frequency components ranging between 0.01 THz to 0.9 THz. To improve the S/N ratio, each projection signal was averaged over 10 iterations. The time-domain signals are Fourier transformed, and the spectral information is extracted for image processing. In order to further improve the S/N ratio, we use the integral of the spectral amplitude over a range of frequencies to reconstruct the image. The chosen spectral range was from 0.05 THz to 0.5 THz ($\lambda \sim 0.6$–6 mm). The spectrally weighted mean wavelength used for image reconstruction is 1.5 mm.

The sub-wavelength output facet of the tapered PPWG produces high-aspect-ratio illumination with a beam profile that is frequency independent in the x direction (across the plates) and frequency dependent in the y direction (parallel to the plates).[6,9,10] In our experiment, the input beam has a Gaussian shape with a beam waist of 1.5 cm at the input face of the PPWG, which is considerably larger than the sample size of 4.5 mm. Therefore, it is reasonable to assume the illuminating intensity to be uniform across the illuminated area on the sample in both x and y directions and take a single signal as an integral of the sample information over the output facet area, including topographic and dielectric information.

Ideally, the inverse radon transform reconstructs the image from line projections. With our tapered-PPWG probe, the line width is determined by the output face in the minor axis direction, which is 20 μm. So, the resulting image obtained from the FBP algorithm is a convolution of the original image with the system point spread function, which is a two-dimensional Gaussian with the spatial extent of the output facet size.[6,15] In the reconstructed image [Fig. 3(b)], the GaAs substrate and antenna features as small as 100 μm can be readily identified. A better resolution ($\sim$20 μm) was not achievable since the sample was not in perfect contact with the output facet.

In conclusion, we used a tapered PPWG as a probe for broad-band THz near-field imaging. The tapered-PPWG probe reflects part of the incident radiation with information from the near field at the output facet. The reflectance is very sensitive to both the topographic and dielectric information of the sample. The FBP algorithm is used to reconstruct the image from the spectral amplitude of the average wavelength of 1.5 mm. Features of size $\sim$100 μm can be qualitatively identified in the reconstructed image.

[1]S. Hunsche, M. Koch, I. Brener, and M. C. Nuss, Opt. Commun. **150**, 22 (1998).
[2]Q. Chen, Z. Jiang, G. X. Xu, and X.-C. Zhang, Opt. Lett. **25**, 1122 (2000).
[3]N. C. J. van der Valk and P. C. M. Planken, Appl. Phys. Lett. **81**, 1558 (2002).
[4]W. L. Chan, J. Deibel, and D. M. Mittleman, Rep. Prog. Phys. **70**, 1325 (2007).
[5]R. Mendis and D. Grischkowsky, Opt. Lett. **26**, 846 (2001).
[6]M. M. Awad and R. A. Cheville, Appl. Phys. Lett. **86**, 221107 (2005).
[7]M. Mbonye, R. Mendis, and D. M. Mittleman, "Study of the impedance mismatch at the output end of a THz parallel-plate waveguide," Appl. Phys. Lett. (submitted).
[8]A. Rusina, M. Durach, K. A. Nelson, and M. I. Stockman, Opt. Express **16**, 18576 (2008).
[9]H. Zhan, R. Mendis, and D. M. Mittleman, Opt. Express **18**, 9643 (2010).
[10]H. Zhan, R. Mendis, and D. M. Mittleman, J. Opt. Soc. Am. B **28**, 558 (2011).
[11]M. Theuer, S. Sree Harsha, and D. Grischkowsky, J. Appl. Phys. **108**, 113105 (2010).
[12]M. Theuer, A. J. Shutler, S. Sree Harsha, R. Beigang, and D. Grischkowsky, Appl. Phys. Lett. **98**, 071108 (2011).
[13]J. Bae, T. Okamoto, T. Fujii, K. Mizuno, and T. Nozokido, Appl. Phys. Lett. **71**, 3581 (1997).
[14]T. Nozokido, N. Miyasaka, and J. Bae, Microwave Opt. Technol. Lett. **53**, 660 (2011).
[15]A. K. Jain, *Fundamentals of Digital Image Processing* (Prentice Hall, Englewood Cliffs, NJ, 1989).
[16]C. A. Balanis, *Advanced Engineering Electromagnetics* (Wiley, New Jersey, 1989).
[17]K. Iwaszczuk, A. Andryieuski, A. Lavrinenko, X.-C. Zhang, and P. U. Jepsen, Appl. Phys. Lett. **99**, 071113 (2011).